
COMBUSTION, EXPLOSION,
AND SHOCK WAVES

Technique for Recording the Intensity of the Emission of Gases behind the Front of Strong Shock Waves in the Region of Vacuum Ultraviolet Radiation

P. V. Kozlov^a, I. E. Zabelinsky^a, N. G. Bykova^a, Yu. V. Akimov^a,
V. Yu. Levashov^{a, *}, G. Ya. Gerasimov^a, and A. M. Teresa^b

^a Institute of Mechanics, Moscow State University, Moscow, Russia

^b Semenov Institute of Chemical Physics, Russian Academy of Sciences, Moscow, Russia

*e-mail: vyl69@mail.ru; levashovvy@imec.msu.ru

Received September 3, 2021; revised March 17, 2022; accepted March 21, 2022

Abstract—A technique for calibrating the recording system for of gas emission behind the shock wave front at the Shock Tube experimental complex of the Institute of Mechanics, Moscow State University in the spectral range 120–185 nm is presented. The presented approach makes it possible to extend the range of obtaining the experimental data to the region of vacuum ultraviolet (VUV) radiation. The study is focused on the issue of obtaining measured values in absolute units. A technique for the preliminary calibration of the measuring system using standard radiation sources is described. It is shown that the power of radiation from the VUV region can significantly exceed the value of radiation fluxes from other regions of the spectrum.

Keywords: shock waves, air radiation, optical system calibration, spectroscopy of atoms and molecules, vacuum ultraviolet radiation

DOI: 10.1134/S1990793122050049

INTRODUCTION

One of the most important practical problems, which designers pay attention to when developing and designing descent vehicles entering the Earth's atmosphere after lunar and later Martian expeditions with the second cosmic velocity, is related to the creation of reliable thermal protection of the surface of the vehicle. As noted in the work [1], increased requirements for the quality of heat-shielding materials and for limiting the weight characteristics of heat-shielding coatings are leading to the need for careful consideration of the problem of heat and mass transfer for new devices. At the same time, the reliability of predicting the degree of heating of the surface of spacecraft under conditions of nonequilibrium heat and mass transfer remains very low to date [2–6]. In the works [7–9], it is noted that with an increase in the velocity of the oncoming flow and the size of the descent vehicle the radiative component of the heat flux increases much faster than the convective one and, starting from the second cosmic velocity, becomes dominant.

The paper [10] presents a method for recording the integral distribution of the shock wave radiation intensity in a wide spectral range (190–1100 nm). However, the radiation power from the vacuum ultraviolet (VUV) region is 120–200 nm, and at high shock wave velocities it turns out to be significantly higher than in

the visible region of the spectrum [11, 12]. However, as noted in the work [13], the component of the radiant heat flux from the VUV region is the least studied. This is due to the fact that VUV radiation is intensely absorbed in the optical path of the spectrometric equipment, and therefore, in order to obtain the corresponding experimental data, it is necessary to use equipment with the preliminary vacuum pumping of the entire internal volume of the spectrometer and the entire radiation output path up to the recording device. Thus, at present there is a need for further efforts in the field of fundamental research on the values of radiative heat fluxes of various gases in a wide range of the spectrum, including in the VUV region. At the same time, in order to build new and validate existing models for calculating nonequilibrium heat transfer, information is needed on the values of radiative heat fluxes in absolute units.

In the works [12, 14], quantitative data are presented on the intensity and time evolution of air radiation behind the front of shock waves in the spectral range of 120 to 400 nm at shock wave velocities of 6.3 to 8.4 km/s. This article is a continuation of the work [10] and contains a description of the procedure for calibrating the measuring system and the technique for recording the intensity of shock-wave radiation in the spectral range of 120 to 185 nm. The experimental data

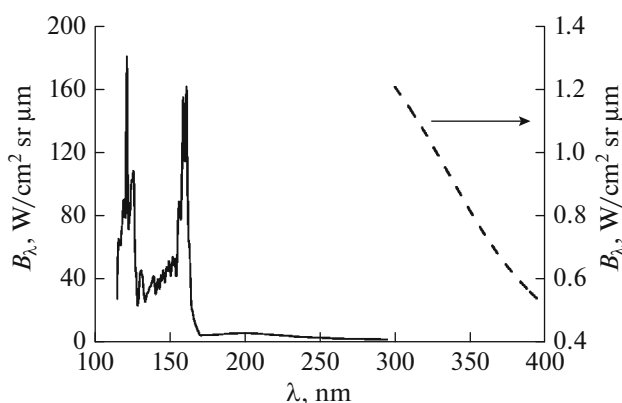


Fig. 1. The emission spectra of a deuterium lamp in the wavelength range of 120 to 400 nm are given by the solid line (data [15]); and those from a SIRSh tungsten lamp, by the dashed line (data from All-Russian Research Institute of Optico-Physical Measurements [16]).

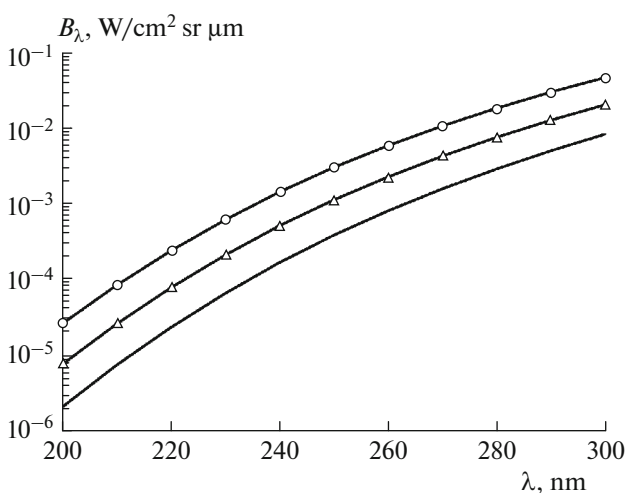


Fig. 2. The emission spectrum of the SIRSh-tungsten lamp8-200 in the wavelength range of 200 to 300 nm for different brightness temperatures: solid line, 2000; Δ , 2100; \circ , 2200°C.

on the radiation of shock-heated gases in the VUV region are presented. The primary attention is paid to the issue of obtaining data in absolute units.

TECHNIQUE OF RECORDING RADIATION IN THE VACUUM ULTRAVIOLET REGION

To obtain experimental information on the radiation intensity in absolute units, it is necessary to preliminarily calibrate the optical system of the experimental setup. For these purposes, a verified reference source of secondary radiation is traditionally used. A deuterium lamp can be used as such a secondary source in the VUV region, but verification of this source is impossible due to the lack of a primary standard at the Russian Institutes of Metrology. In this

case, the reference source for the VUV region is usually calibrated by comparing its emission intensity with the emission intensity of the secondary calibrated standard in the common ultraviolet range for these two sources. To extend the data to the VUV range, it is assumed that the shapes of the emission spectra of all deuterium lamps are similar. As the initial data on the spectral brightness of the radiation of a deuterium lamp in the wavelength range $\lambda = 115\text{--}300$ nm, in this study, we use data on the emission spectrum of a McPherson (United States) lamp model 632 [15] and data from the All-Russian Research Institute of Optico-Physical Measurements [16]. The spectra of the McPherson deuterium lamp in the range $\lambda = 120\text{--}300$ nm (solid line) and the SIRSh tungsten lamp in the range $\lambda = 300\text{--}400$ nm (dashed line), taken with a spectral resolution of 0.8 nm, are shown in Fig. 1.

To determine the intensity of the spectrum of a particular deuterium lamp, the region of its spectrum which overlaps the emission spectrum of the secondary reference source in the UV region ($\lambda > 250$ nm) is used. A lamp with a tungsten filament (for example, a SIRSh-8-200 lamp) heated to a brightness temperature above 2000°C can be used as such a source. From a comparison of the radiation intensity of both lamps at the selected wavelength λ_0 , we can obtain the conversion factor used later to calculate the radiation intensity of a deuterium lamp in the rest of its spectra, taking into account the assumption that the shape of the radiation spectrum of all deuterium lamps is similar. The emission spectra of a tungsten filament for several values of the brightness temperature are shown in Fig. 2.

The emission spectra of tungsten and deuterium lamps were compared according to the optical scheme shown in Fig. 3. When a deuterium lamp was installed in the optical circuit, the entire optical path was preliminarily completely evacuated. As the experimental data showed, this requirement is an important condition, since the ozone formed in the air under the action of ultraviolet radiation is a powerful absorber of UV and VUV radiation. When a tungsten lamp is used as the radiation source, the preliminary pumping out of the optical path is not required, since the intensity of its radiation in the ultraviolet region is several orders of magnitude lower than that of a deuterium lamp.

In this scheme (Fig. 3), no additional optical elements (lenses, mirrors) are used on the optical axis between the radiation source and the inlet slit of the VM-1 vacuum monochromator. The absence of focusing elements in the optical scheme leads to the need to take into account the difference in the sizes of the radiation sources used, as well as the geometric dimensions of the exit slit on the shock tube and the inlet slit of the monochromator. The deuterium source is a gas-discharge cylinder, the radiation from which passes through the diaphragm, which is a circle with diameter $D_D = 3$ mm; the tungsten filament of the

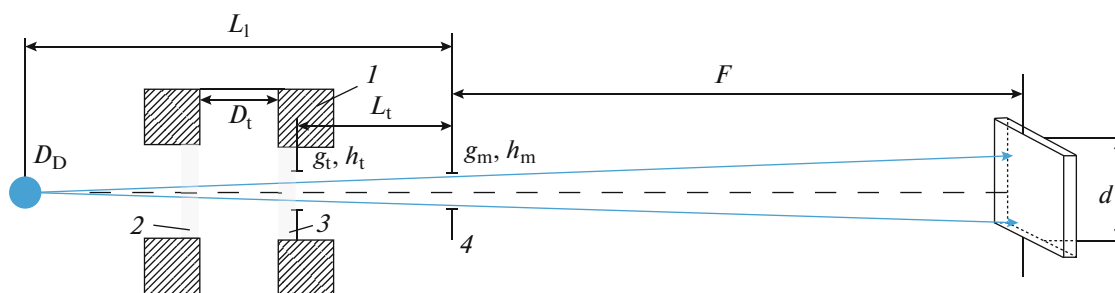


Fig. 3. Optical scheme for calibrating the radiation of a deuterium lamp: I , section of the shock tube in the measuring section; 2, 3, magnesium fluoride windows; 4, inlet slit of the vacuum monochromator; D_D , aperture of deuterium lamp; g_t and h_t are the width and height of the slit at the exit window of the shock tube; g_m and h_m are the width and height of the inlet slit of the monochromator; D_t is the internal diameter of the shock tube; L_1 is the distance from the deuterium lamp to the inlet slit of the monochromator; L_t is the distance from the inner surface of the tube to the monochromator; F is the focal length of the monochromator; d is the height of the diffraction grating of the monochromator.

SIRSh lamp has a width of $g_w = 2$ mm and height of $h_w = 10$ mm. The width (g_t) and height (h_t) of the slit on the shock tube were 0.22 and 8 mm, respectively. The width (g_m) and height (h_m) of the input monochromator slits were 0.25 and 20 mm. The width of the lamp region, the radiation from which enters the monochromator (g_1), is determined by the expression

$$g_1 = g_t + \frac{(g_t + g_m)(L_1 + L_t)}{2L_t},$$

where L_1 is the distance from the radiation source to the inlet slit of the monochromator and L_t is the distance from the inner surface of the tube to the inlet slit of the monochromator. For the parameters of the circuit used in the calibration, the value g_1 is 0.39 mm, which for both lamps is smaller than the dimensions of the sources in the horizontal direction (source width). At the same time, the height of the detected area of the source is limited only by its vertical dimensions, which are 3 mm in the case of a deuterium lamp and 10 mm in the case of a tungsten lamp. The intensity of radiation entering the monochromator and radiation recorded by the detector at the selected wavelength is determined from the following expression:

$$I_1 = B_1 S_1 \Omega_1 \delta \lambda, \quad (1)$$

where B_1 is the spectral energy brightness of the lamp [$\text{W}/\text{cm}^2 \text{sr km}$]; S_1 is the area of the lamp area, the radiation from which enters the monochromator [cm^2]; Ω_1 is the solid angle, which is determined by the optical scheme used [sr]; and $\delta \lambda$ is the spectral range (wavelength range) extracted by the monochromator [μm].

The area of the lamp, the radiation from which enters the monochromator, S_1 , for deuterium (S_D) and tungsten (S_W) lamps is determined by the following expressions:

$$S_D = D_D g_1, \quad (2)$$

$$S_W = h_w g_1. \quad (3)$$

The solid angle Ω_1 is calculated from the distance from the emitting object to the inlet slit of the monochromator (L_1), monochromator inlet slit width (g_m), and height (h_0) of the limiting aperture of the optical scheme in the plane of the inlet slit of the monochromator:

$$\Omega_1 = \frac{g_m h_0}{L_1^2}. \quad (4)$$

Value h_0 is determined by the smallest of the three angles: (1) by the angle determined by the height of the slit on tube h_t and the difference in the distance between L_1 and L_t , i.e. $(L_1 - L_t)$; (2) by the angle calculated from the height of the inlet slit of the monochromator h_m and distance L_1 ; (3) by the angle determined by the height of the diffraction grating of the monochromator (d) and distance $L_1 + F$. This smallest angle (α) and the distance corresponding to the given angle (L) allows us to determine the height of the limiting aperture from the following expression: $h_0 = \alpha L$.

The radiation intensity of the deuterium lamp, I_D , in the investigated spectral range can be obtained by multiplying the values obtained in the experiment with a deuterium lamp I_D^{exp} [mV] by the inverse sensitivity function of the optical circuit. The sensitivity of the optical scheme, in turn, is determined from the experiment with a tungsten lamp as the ratio of the radiation intensity of the latter in absolute units, I_W [W], to its intensity measured in the experiment, I_W^{exp} . Figure 4 shows the data on the radiation intensities of deuterium (I_D^{exp}) and tungsten (I_W^{exp}) lamps, measured in experimental units (hereinafter, referred to as units of *ex-ta*), for the wavelength range of 220 to 320 nm. Thus, the radiation intensity of a deuterium lamp is determined by the following expression:

$$I_D = \frac{I_D^{\text{exp}}}{I_W^{\text{exp}}} I_W. \quad (5)$$

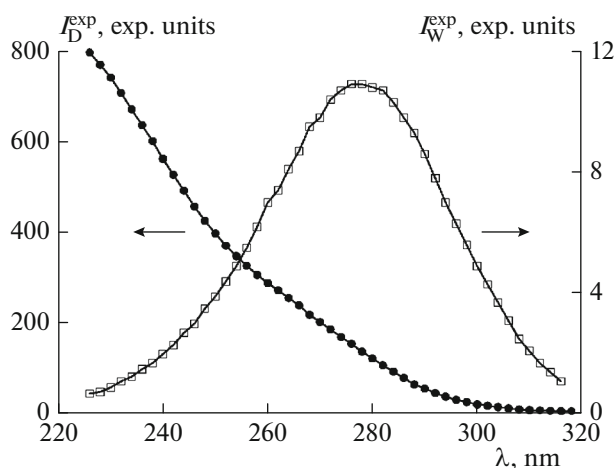


Fig. 4. The measured radiation intensities of the deuterium lamp (\bullet) and SIRSh lamps (\square) in units. ex-ta.

Using expressions (1)–(5) and the height of the limiting aperture h_0 , we can obtain the following expression for the spectral energy brightness of a deuterium lamp:

$$B_D = \frac{B_W h_W I_D^{\text{exp}}}{I_W^{\text{exp}} D_D}. \quad (6)$$

The plot of the inverse sensitivity of the optical design, i.e., relations I_W/I_W^{exp} , obtained in an experiment with a tungsten lamp is shown in Fig. 5.

The approach described above makes it possible to determine the magnitude of the spectral energy brightness of a specific (used) deuterium lamp for the VUV region. The results of preliminary calibration

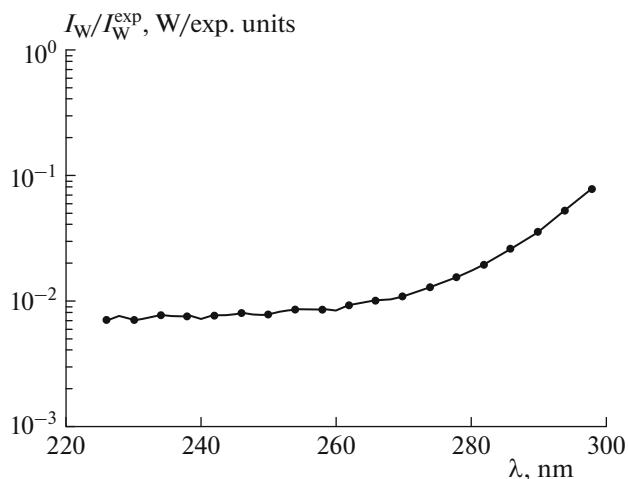


Fig. 5. The sensitivity of the optical circuit of the SIRSh tungsten lamp.

experiments with the Hamamatsu L879 deuterium lamp used are shown in Fig. 6. For comparison, the same figure shows data on the spectral energy brightness of a McPherson model 632 deuterium lamp. As can be seen from this figure, in the considered spectral range, the brightness of the Hamamatsu L879 deuterium lamp used is less than the brightness declared for the McPherson model 632 deuterium lamp by a factor of about 2.5.

It should be noted here that since the calibration experiments were carried out in the wavelength range (~ 300 nm), where the spectra of both lamps change smoothly, the coefficient obtained does not depend on the instrumental function of the optical scheme. In contrast, in the wavelength range of 120–170 nm, sharp structures are observed in the spectrum of a deuterium lamp (see Fig. 1), the value of the intensity maximums of which depends on the spectral width of the instrumental function of the monochromator. Therefore, in addition to applying the conversion factor to the original spectrum, it is necessary to recalculate it for a specific hardware function. In our experiments, the half-width of the instrumental function (0.85 nm) practically coincided with the spectral resolution declared for the initial spectrum of the deuterium lamp (0.8 nm), which did not require additional correction of the spectrum.

The procedure described above makes it possible to obtain a calibrated secondary radiation source for the VUV region, which is subsequently used for calibration of the optical system of the experimental setup. The performed calibration procedure makes it possible to obtain experimental data on the radiation intensity of shock-heated gases in the VUV region in absolute units. Examples of such measurements are presented in Figs. 7–9.

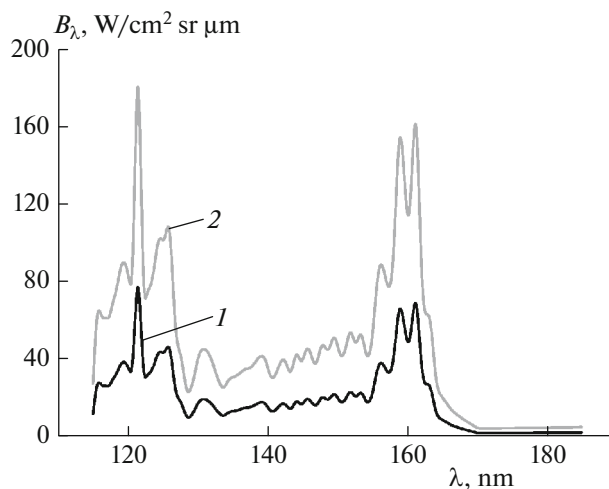


Fig. 6. Emission spectra of calibrated deuterium lamp (1) and McPherson lamp (2) for the wavelength range of the spectrum 115–185 nm.

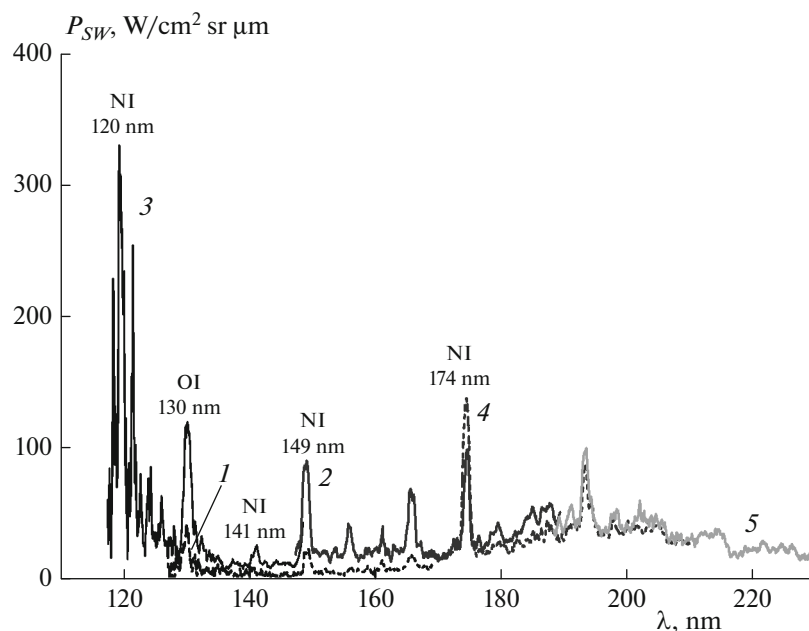


Fig. 7. Spectral energy density of shock wave radiation in air at initial pressure $P_1 = 0.25$ Torr and various shock wave velocities V_{SW} , km/s: 1, 6.5; 2, 7.0; 3, 7.2; 4, 8.2; 5, 8.4 km/s.

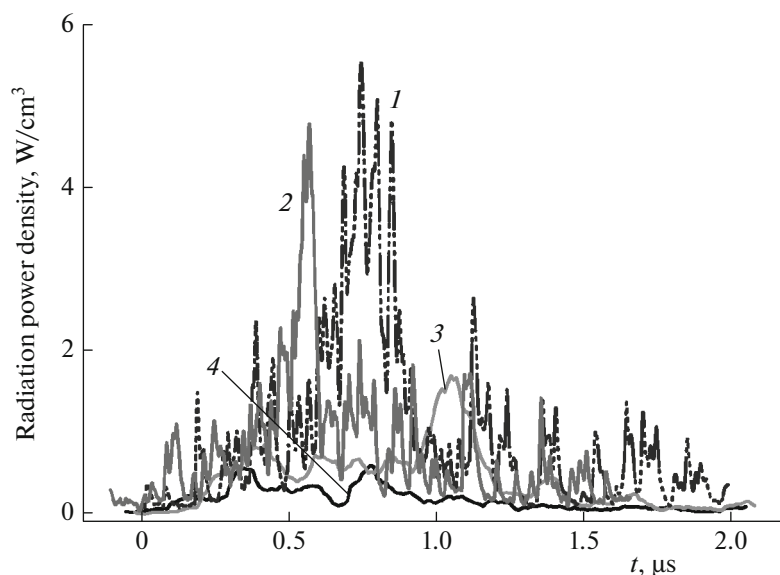


Fig. 8. Temporal evolution of the power density of the shock wave radiation in air for different wavelengths and velocities: $V_{SW} = 8.73$ (1) and 8.39 km/s (2) for $\lambda = 120$ nm; $V_{SW} = 9.07$ (3) and 7.72 km/s (4) for $\lambda = 130$ nm.

Figure 7 shows the panoramic spectrum of the radiation of the shock wave in air in the range $\lambda = 120$ – 185 nm for various shock wave velocities: 6.5–8.4 km/s. This spectrum is the integral radiation recorded by the measuring equipment for the effective time of shock wave radiation [10]. As can be seen from the spectrum given above, in the radiation of a shock wave in air in the VUV region, there is one resonance line of the oxygen atom at a wavelength of 130 nm and several

lines of the nitrogen atom, namely, multiplets at $\lambda = 120$, 141, 149, and 174 nm. In this case, the value of the measured integral radiation near $\lambda \approx 120$ nm is several times higher than the amount of radiation in the range $\lambda = 130$ – 220 nm. This also confirms the need to obtain information on the values of radiative heat fluxes from the VUV region.

It should be noted that the panoramic radiation spectrum provides general information about the

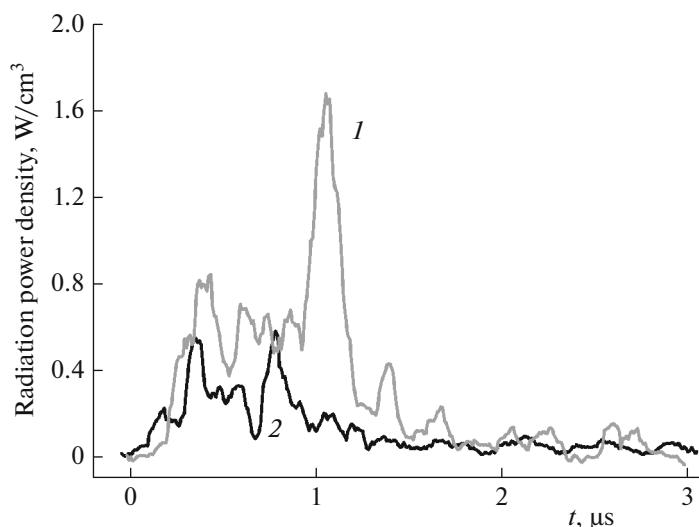


Fig. 9. Temporal evolution of the power density of shock wave radiation in air at a wavelength of 130 nm for various shock wave velocities: 1, $V_{SW} = 9.07$ km/s; 2, $V_{SW} = 7.72$ km/s.

nature of the shock-heated gas spectrum, and also makes it possible to determine the wavelength regions of interest for research. In this case, the duration of radiation of individual components of the shock-heated gas can differ significantly. As a consequence, to correctly determine the radiation power, it is also necessary to study its temporal characteristics with a sufficient (nanosecond) resolution [10]. Figures 8 and 9 show oscillograms of the time evolutions of the radiation power density in the narrow, selected spectral range. The moment of time $t = 0$ μ s on the time scale corresponds to the moment when the gas-dynamic front arrives at the optical axis of observation.

Figure 8 shows the time evolution of the radiation power in air at wavelengths of 120 and 130 nm for various shock wave velocities. Figure 8 shows that the maximum value of the radiation intensity strongly depends on the wavelength. For example, the maximum radiation intensity at a wavelength of 120 nm is approximately twice the same value at a wavelength of 130 nm. In this case, the shock wave velocities are approximately the same in both cases.

The effect of the shock wave velocity on the intensity and duration of radiation is shown in Fig. 9. Here the time evolutions of the radiation intensity at a wavelength of 130 nm are given for two shock wave velocities. It can be seen from this figure that an insignificant increase in the shock wave velocity (by a factor of 1.17) leads to a significant change in the maximum radiation value (by a factor of 3.2).

Thus, only the joint use of the panoramic spectrum data and the results of time evolutions in a narrow spectral range can provide correct information on the power density of radiation from various plasma components resulting from the passage of a shock wave.

CONCLUSIONS

The article is a continuation of [10] and extends the studied spectral range to the region of VUV radiation. The paper describes a technique for calibrating an optical system to obtain data on the radiation of a shock-heated high-temperature gas from the VUV region (120–185 nm). For these purposes, a deuterium lamp is used in the study. In this case, to determine the intensity of the spectrum of a particular deuterium lamp, the region of its spectrum is used, which overlaps with the emission spectrum of the secondary reference source in the UV region ($\lambda > 250$ nm). A lamp with a tungsten filament was used as such a source. The performed calibration procedure makes it possible to obtain experimental data on the radiation intensity of shock-heated gases in the VUV region in absolute units. Examples of such measurements are given.

FUNDING

This study was carried out as part of the scientific plan of the Institute of Mechanics of Moscow State University (no. AAAA-A19-119012990112-4) with the support of the Russian Foundation for Basic Research (grant no. 20-08-00343).

REFERENCES

1. V. I. Vlasov, G. N. Zalogin, V. V. Lunev, and D. A. Churakov, *Fiz.-Khim. Kinet. Gaz. Dinam.* **13** (1) (2012). <http://chemphys.edu.ru/No.s/2012-13-2/articles/306/>
2. S. T. Surzhikov and M. P. Shuvalov, *High Temp.* **51**, 408 (2013).
3. A. M. Brandis, C. O. Johnston, and B. A. Cruden, in *Proceedings of the 16th AIAA Thermophysics Conference* (AIAA, VA, 2016), AIAA-2016-3690.

4. C. O. Johnston, B. R. Hollis, and K. Sutton, *J. Spacecr. Rockets* **45**, 1185 (2008).
5. D. R. Olynick, W. D. Henline, L. C. Hartung, and G. V. Candler, in *Proceedings of the 6th AIAA ASME Jt. Thermophys. Heat Transfer Conference* (AIAA, VA, 1994), AIAA 94-1955.
6. S. T. Surzhikov, *Russ. J. Phys. Chem. B* **2**, 800 (2008).
7. H. Wei, R. G. Morgan, T. J. McIntyre, A. M. Brandis, and C. O. Johnston, in *Proceedings of the 47th AIAA Thermophysics Conference* (AIAA, VA, 2017), AIAA 2017-4531.
8. C. O. Johnston and A. M. Brandis, *J. Spacecr. Rockets* **52**, 105 (2015).
9. S. Surzhikov, in *Proceedings of the 55th AIAA Aerospace Scientific Meeting* (AIAA, VA, 2017), AIAA 2017-1147.
10. P. V. Kozlov, I. E. Zabelinskii, N. G. Bykova, Yu. V. Akimov, V. Yu. Levashov, G. Ya. Gerasimov, and A. M. Tereza, *Russ. J. Phys. Chem. B* **15**, 652 (2021).
11. B. Cruden, R. Martinez, J. Grinstead, and J. Olejniczak, in *Proceedings of the 41st AIAA Thermophysics Conference* (AIAA, VA, 2009), AIAA 2009-4240.
12. N. G. Bykova, I. E. Zabelinskii, L. B. Ibragimova, P. V. Kozlov, S. V. Stovbun, A. M. Tereza and O. P. Shatalov, *Russ. J. Phys. Chem. B* **12**, 108 (2018).
13. S. L. Gorelov and A. Yu. Kireev, *Fiz.-Khim. Kinet. Gaz. Din.* **15** (1) (2014). <http://chemphys.edu.ru/No.s/2014-15-1/articles/77/>.
14. N. G. Bykova, I. G. Gerasimov, I. E. Zabelinskii, L. B. Ibragimova, and O. P. Shatalov, *Fiz.-Khim. Kinet. Gaz. Din.* **15** (2) (2014). <http://chemphys.edu.ru/No.s/2014-15-2/articles/114/>.
15. Hamamatsu Deuterium Lamps D2 LAMPS. www.hamamatsu.com/resources/pdf/etd/D2lamps_TLS1017E.pdf. Accessed 2020.
16. www.vniiofi.ru/.